


# Impact of resource allocation on information-disease coupled propagation considering node importance in multiplex networks

Liang'an Huo(霍良安), Jiaxue Cha(查佳雪), and Yue Yu(于跃)
**Citation:**Chin. Phys. B, 2026, 35 (**7**): 078903. DOI: 10.1088/1674-1056/ae31da
http://cpb.iphy.ac.cn; http://iopscience.iop.org/cpb

**What follows is a list of articles you may be interested in**

---

## A node importance prediction algorithm based on graph attention and contrastive learning

Jun Ai(艾均), Yuming Zhang(张玉明), Zhan Su(苏湛), Chenye Guo(郭晨晔), and Mingsong Li(李铭松)
Chin. Phys. B, 2026, 35 (**5**): 058901. DOI: 10.1088/1674-1056/ae0680

## Influence of negative information dissemination and vaccination behavioral decision-making on epidemic spreading in a three-layer network

Liang’an Huo(霍良安) and Leyao Yin(尹乐瑶)
Chin. Phys. B, 2025, 34 (**6**): 068902. DOI: 10.1088/1674-1056/adc402

## AIGCrank: A new adaptive algorithm for identifying a set of influential spreaders in complex networks based on gravity centrality

Ping-Le Yang(杨平乐), Lai-Jun Zhao(赵来军), Chen Dong(董晨),Gui-Qiong Xu(徐桂琼), and Li-Xin Zhou(周立欣)
Chin. Phys. B, 2023, 32 (**5**): 058901. DOI: 10.1088/1674-1056/ac8e56

## Contagion dynamics on adaptive multiplex networks with awareness-dependent rewiring

Xiao-Long Peng(彭小龙) and Yi-Dan Zhang(张译丹)
Chin. Phys. B, 2021, 30 (**5**): 058901. DOI: 10.1088/1674-1056/abe1ab

## Shortest path of temporal networks: An information spreading-based approach

Yixin Ma(马一心), Xiaoyu Xue(薛潇雨), Meng Cai(蔡萌), and Wei Wang(王伟)
Chin. Phys. B, 2020, 29 (**12**): 128902. DOI: 10.1088/1674-1056/abb302

---

# Impact of resource allocation on information–disease coupled propagation considering node importance in multiplex networks

Liang'an Huo(霍良安)[1,2,†], Jiaxue Cha(查佳雪)[1], and Yue Yu(于跃)[1]

[1] *Business School, University of Shanghai for Science and Technology, Shanghai* 200093, *China*
[2] *School of Intelligent Emergency Management, University of Shanghai for Science and Technology, Shanghai* 200093, *China*

(Received 15 September 2025; revised manuscript received 14 November 2025; accepted manuscript online 30 December 2025)

During a large-scale epidemic outbreak, effective resource allocation is vital for controlling disease transmission. Prioritizing resource provision to communities experiencing severe infections can mitigate further spread, while prioritizing information dissemination to influential individuals can expand the publicity effect. This paper proposes a novel two-layer information–disease transmission coupled model that optimizes the allocation of information and medical resources based on node importance analysis, aiming to explore the synergistic effects of resource allocation on disease dynamics. The study employs the microscopic Markov chain approach to construct dynamic equations and derive the epidemic threshold, with Monte Carlo simulations used to validate the theoretical results. Findings demonstrate that expanding the scope of preventive information dissemination through mass media improves public awareness of disease prevention and significantly curbs epidemic transmission. Moreover, reducing the resource deployment threshold in infected communities enables more precise resource allocation during the early stages of an outbreak, which is vital for increasing the epidemic threshold and reducing the final size of the epidemic. These findings provide robust theoretical foundations and actionable guidelines for optimizing resource allocation strategies in public health emergency management.

**Keywords:** information dissemination, disease transmission, resource allocation, node importance, multilayer network

**PACS:** 89.75.–k, 87.23.Ge, 87.19.X–

**DOI:** 10.1088/1674-1056/ae31da **CSTR:** 32038.14.CPB.ae31da

## 1. Introduction

The outbreak of COVID-19 posed a severe challenge to humanity, not only seriously jeopardizing human health and resulting in a high mortality rate[1–3] but also triggering a series of cascading effects in multiple dimensions, such as economic,[4,5] social[6] and so on. These impacts have led to profound and far-reaching negative consequences that are far more detrimental than the disease itself. An in-depth understanding of the transmission mechanisms and influencing factors of large-scale disease outbreaks is of vital significance for effectively controlling epidemic spread and reducing losses to human societies.[7,8] Over the years, there has been a wealth of academic research on disease transmission modeling. As early as 1927, Kermack and McKendrick[9] first proposed the threshold theory in infectious disease dynamics by developing the susceptible–infected–removed (SIR) model. They then extended this to the susceptible–infected–susceptible (SIS) model for diseases that have no long-term immunity or where immunity declines over time. Nekovee *et al.*[10] unified the Maki–Thompson model with the SIR epidemic model and established the rumor-spreading SIS (ignorer–spreader–silent) model to simulate the dynamic spreading process of rumors in complex social networks. Since then, research on information and disease propagation has been continuously developed and enriched. Gómez *et al.*[11] pioneered the microscopic Markov chain approach (MMCA) for analyzing the spread of contact-based diseases in complex networks. Building upon this foundation, Granell *et al.*[12] proposed a multiplex network model to investigate the dynamic coupling between disease transmission and information dissemination, using the MMCA for theoretical analysis and deriving the epidemic outbreak threshold. Subsequent studies have built on this foundation by adding the effect of mass media, a massive spread of awareness, and the degree of immunity to disease.[13] Sun *et al.*[14] investigated the effect of mass media in an SIRS–UAU (unaware–aware–unaware) disease-awareness spreading model. Zhu *et al.*[15] developed a three-layer network model to explore the interaction among information diffusion, awareness, and green behavior spreading. Bao and He[16] introduced positive and negative information and time delays to analyze their effects on disease transmission. Based on the consideration of advection effects, Yang *et al.*[17] established a corresponding infectious disease transmission model incorporating delay effects. Han and Wang[18] found that denser community structure and increased inter-community connectivity contributed to the spread of awareness. Zhou *et al.*,[19] on the basis of a time-varying two-layer network model, proposed two strate-

[†]Corresponding author. E-mail: huohuolin@yeah.net

© 2026 Chinese Physical Society and IOP Publishing Ltd. All rights, including for text and data mining, AI training, and similar technologies, are reserved.

gies — avoiding and reducing behavioral strategies — and investigated their impact on an epidemic. Liu *et al.*,[20] by extending the SIS model, studied the coupled dynamics of multi-strain disease and negative vaccine information. These studies yielded critical insights into disease transmission dynamics and established a robust scientific foundation for advancing epidemiological theories and optimizing evidence-based public health interventions.

During epidemic outbreaks, healthcare resources are crucial to patient recovery and the protection of susceptible populations. Resource scarcity can significantly exacerbate disease transmission.[21] Research findings[22,23] have demonstrated that optimizing resource allocation through rational utilization types and allocation strategies can significantly enhance the containment of disease outbreaks. Chen *et al.*[24] proposed a coupling model of resource allocation and disease transmission by considering the impact of individual self-awareness on resource allocation. Wang *et al.*[25] constructed a multilayer network to explore the relationship between resource allocation, information dissemination, and disease transmission. As a resource, information also plays an important role in disease transmission. Huo and Zhao[26] constructed a coupling model of consciousness and disease transmission, considering the influence of information resources and medical resources, and found that both exert a strong inhibitory effect on disease spread, while Yu and Huo[27] established a four-layer network communication model to study the co-evolution of information dissemination, behavioral adoption, resource transfer, and disease transmission.

In the context of real-world scenarios where resource availability is constrained, the prioritization of resource allocation to key population groups assumes critical importance during epidemic outbreaks.[28] Meng *et al.*[29] assessed node importance based on various factors, including degree centrality, and proposed an optimized vaccination strategy. Chen *et al.*[30] demonstrated that epidemic spread is influenced by prioritized resource allocation and proposed a strategy of prioritizing the allocation of medical resources to highly infectious nodes at an early stage. Wang *et al.*[31] examined resource allocation strategies considering node degree preference and local sensitivity density, identifying the optimal and suboptimal strategies under different scenarios. In the realm of information resources, Liu *et al.*[32] ranked node influence in asymmetric interaction multiplex networks and identified influential spreaders to control epidemic diffusion. Xian *et al.*[33] disseminated mass media information to high-degree nodes and found that increasing the proportion of dissemination exerted a stronger inhibitory effect on disease spread.

Existing studies seldom cover information resources and predominantly focus on the allocation of medical resources, often assuming them equally accessible to all individuals. Under rapid disease outbreaks, both information and medical resources must be strategically allocated to critical nodes within networks to maximize their effectiveness.

Information resources are accessible through multiple channels, such as online mass media and offline community promotion. In virtual networks, the varying importance of nodes is reflected in individuals' differing capacities to disseminate information after receiving it. Consequently, mass media strategically allocate information resources to individuals with high "degree" rankings in information networks, leveraging their superior capacity for rapid information diffusion. In offline networks, publicity on epidemic prevention in high-infection communities is often more important, as nodes in these communities face a greater risk of infection. Therefore, prioritizing information resource provision to individuals in these communities is important to prevent the spread of an epidemic.

Medical resources are also accessible through multiple channels, including centralized allocation systems that distribute them to residents through community-level infrastructures. As epidemiological units, communities exhibit differential levels of infection due to population density gradients and mobility patterns. In disease transmission networks, nodes in high-infection communities face greater demand due to elevated infection risk and treatment needs, thereby increasing their importance. In response, communities implement needs-based resource allocation, prioritizing areas with a high infection rate to address urgent demands for epidemic containment and patient care.

To model this process, this study constructs a two-layer network coupled model that accounts for both informational and medical resource allocation. One layer represents the dissemination of information driven by mass media and the other captures the distribution of medical resources driven by communities. The main points of innovation are as follows:

(i) Treating information as a virtual resource and considering the limited availability of medical and information resources, we investigate the coupled effects of rational resource allocation on information–disease transmission.

(ii) We propose a new information resource allocation strategy. Mass media allocate online information resources to individuals with superior "degree" rankings in the information dissemination layer, while individuals within high-infection communities also acquire offline information resources through communities in the disease transmission layer.

(iii) For allocating medical resources, we consider the actual community environment where individuals reside. A new demand-based medical resources allocation strategy prioritizes resource allocation to communities with a higher in-

fection rate in the disease transmission layer, thereby meeting the pressing needs for prevention and treatment.

The paper is organized as follows: Section 2 develops the two-layer network framework, Section 3 analytically derives the epidemic threshold using MMCA, Section 4 examines parameter effects through simulation, and Section 5 presents concluding remarks.

## 2. Model design

During the COVID-19 pandemic, mainstream media utilized online platforms to promptly disseminate pandemic updates and prevention information. Meanwhile, some online opinion leaders — typically with substantial follower networks — reposted and contextualized these official authoritative updates, improving the dissemination efficiency and public acceptance of pandemic-related information.[34] Analogous to the effect of celebrity endorsements in augmenting product exposure, they draw substantial public attention.[35] In densely populated offline communities, epidemic prevention information is frequently and comprehensively publicized through mobile publicity and fixed-point broadcasting. Additionally, the government implemented a centralized procurement and allocation system for material distribution in lockdown zones and high-risk infection areas to minimize interpersonal contact and reduce infection risks. This model, organized at the community level, delivered medical resources such as testing kits and medication packages directly to residents.[36,37] By emphasizing precision in resource allocation, particularly within communities with high infection rates, this approach effectively addressed urgent medical needs and contributed to curbing viral transmission.

This paper constructs an information–disease (UAU–SIS) two-layer network model, as shown in Fig. 1, where the nodes in the upper and lower layers are in one-to-one correspondence. The first layer is the information dissemination layer with two types of node states, aware (A) and unaware (U), which indicate awareness or lack of awareness of the disease information, respectively. The information dissemination layer configures mass media as an information allocation source to simulate official epidemic prevention publicity through mass media's online channels. The second layer is the disease transmission layer, and there are two types of node states, which indicate susceptibility (S) to the disease and being infected (I) with the disease, respectively. Nodes in this layer are categorized into multiple communities, with interconnections predominantly concentrated within the same communities. Such community networks mirror people's behavioral patterns of greater propensity for interaction with members within their own communities. At the same time, a medical resource allocation center is set as a resource allocation source to disseminate information about epidemic prevention and distribute medical resources in communities with high infection rates.

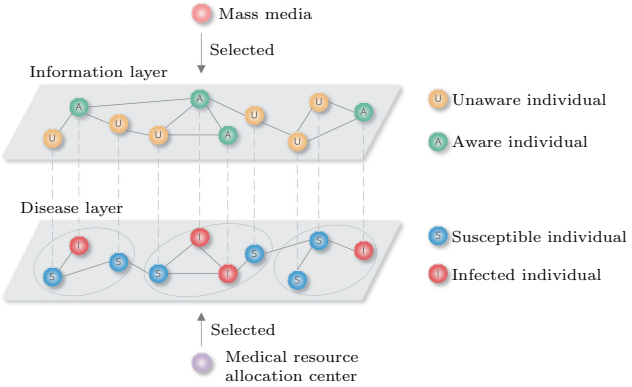



**Fig. 1.** UAU–SIS model.

### 2.1. Information dissemination process

In the information dissemination layer, A-state individuals are aware of the disease-related information and transmit a certain amount of information to their connected U-state neighbors within a certain time. A U-state individual $i$ becomes informed with probability $\lambda_i(t)$, and an A-state individual $j$ may forget the information and revert to state U with probability $\delta_j(t)$. Both probabilities $\lambda_i(t)$ and $\delta_j(t)$ are affected by the amount of information resources an individual possesses.




**Fig. 2.** UAU state transition diagram.

Information resources refer to the cumulative amount of information an individual receives through multiple network channels, exhibiting a cumulative social reinforcement effect. In this paper, we utilize "unit" as the measure to quantify the volume of information resources. Accumulation of information resources enhances an individual's understanding of specific events such as epidemics. With broader access, individuals can fully grasp the severity, transmission and prevention methods, which fosters trust in the information and lowers resistance to it. A U-state individual $i$ is informed with the probability $\lambda_i(t)$, and an A-state individual $j$ may forget the information then revert to state U with the probability $\delta_j(t)$. Individuals armed with rich information can construct a systematic knowledge framework of the disease. Using this information to guide protective behaviors leads to memories that are both more durable and slower to decay. Consequently, the more information resources an A-state individual $j$ has, the more it can slow down the forgetting of information, and thus the forgetting rate $\delta_j(t)$ will be lower. At time step $t$, the probability

$\lambda_i(t)$ of node $i$ receiving information in state U and the probability $\delta_i(t)$ of node $j$ forgetting information in state A are defined as follows:

$$\lambda_i(t) = \xi_1 \left[1 - \lambda (1-\varepsilon_1)^{M_i(t)}\right], \tag{1}$$

$$\delta_j(t) = \xi_2 \delta \varepsilon_2^{M_j(t)}. \tag{2}$$

In this context, $\lambda$ denotes the level of accessibility of information resources, where an increase in $\lambda$ indicates greater difficulty in receiving the information resources. $\varepsilon_1$ and $\varepsilon_2$, respectively, represent the information assimilation utilization rate and memory decay utilization rate. $M_i(t)$ refers to the information resources of node $i$ at time step $t$, while $\xi_1$ and $\xi_2$ serve as moderating factors. $\delta$ denotes the initial forgetting rate.

Individuals access information resources through multiple channels. In this paper, online mass media and medical resource allocation are designated as the primary sources of information, both of which are selective in their dissemination. For the online nodes, they are ranked according to their degree. We use $Q_i$ to represent the degree ranking of node $i$ in the information dissemination layer. At each time step, mass media disseminate one unit of information resources to individuals with the ratio of degree ranking $Q_i/N$ within $\eta_1$, where $N$ represents the number of nodes in the information dissemination layer. For offline communities, the infection rates are calculated for each community. There are $k$ communities (denoted as $H_1, H_2, \ldots, H_k$), where community $H_k$ contains $N_{H_k}$ nodes. As the epidemic progresses, different communities exhibit different and dynamically evolving infection statuses, with the specific process illustrated in Fig. 3.

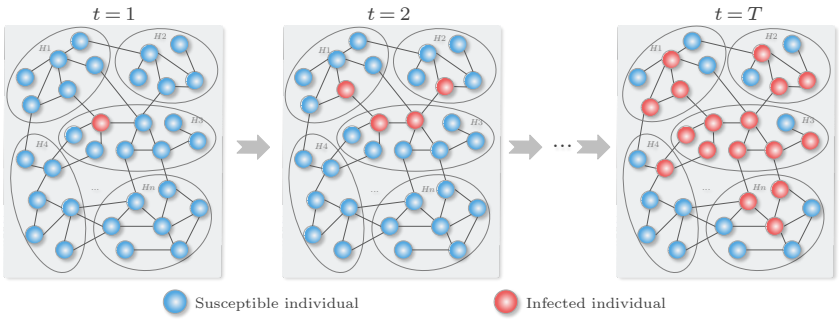



**Fig. 3.** Diagram of community infection dynamics.

We use $N^{\mathrm{I}}_{H_k}(t)/N_{H_k}$ to represent the infection rate in community $H_k$ of the disease transmission layer at time step $t$, where $N^{\mathrm{I}}_{H_k}(t)$ represents the number of infected nodes in community $H_k$ at time step $t$. We define communities with infection rates exceeding $\eta_2$ as high-risk communities; these require epidemic prevention campaigns. At each time step, all individuals in these communities receive one unit of information resources from their respective communities. It is also assumed that an A-state individual generates one unit of information resources within each time step, then shares all its information resources with its online U-state neighbors while maintaining its own information resource quantity unchanged. Because the U-state individual is unaware of the information about the disease, it receives less information than the A-state individual, who fully receives one unit of information resource. For this reason, a decay factor $\gamma$ is set. And when individuals are exposed to community outreach campaigns, they tend to perceive a closer subjective psychological distance to regions severely affected by the disease and demonstrate heightened accessibility to informational resources. Therefore, the decay factor $\gamma_1$ for the reception of information resources from online media is smaller than the decay factor $\gamma_2$ for the reception of information resources from community outreach.

Within each time step, the information resource quantity source of an A-state individual is: (i) one unit of information generated by each A-state individual themselves; (ii) one unit of information resource disseminated by mass media, if the A-state individual ratio of degree ranking $Q_i/N$ is within $\eta_1$; (iii) one unit of information resource from their respective communities, if A-state individuals are in communities with infection rate $N^{\mathrm{I}}_{H_k}(t)/N_{H_k}$ exceeding $\eta_2$. To describe this phenomenon, we introduce the Heaviside step function $F(x)$. When $x \geq 0$, $F(x) = 1$; otherwise $F(x) = 0$. For node $i$ belonging to community $H_k$, the information resource quantity for individuals in state $A$ is specifically defined as follows:

$$\underset{i\in H_k}{M^{\mathrm{A}}_i}(t) = 1 + F\left[\eta_1 - \frac{Q_i}{N}\right] + F\left[\frac{N^{\mathrm{I}}_{H_k}(t)}{N_{H_k}} - \eta_2\right]. \tag{3}$$

Within each time step, the information resource quantity source of a U-state individual is: (i) the sum of information resources $\sum_j a_{ij} P^{\mathrm{A}}_j(t) M^{\mathrm{A}}_i(t) / \sum_{l\neq i} a_{jl} P^{\mathrm{U}}_l(t) + 2$ shared by all A-state neighbors; (ii) $\gamma_1$ units of information resource disseminated by mass media if the U-state individual ratio of degree ranking $Q_i/N$ is within $\eta_1$; (iii) $\gamma_2$ units of information resource from their respective communities if U-state individu-

als are in communities with infection rate $N^{\mathrm{I}}_{H_k}(t)/N_{H_k}$ exceeding $\eta_2$. Similarly, we introduce the Heaviside step function $F(x)$ for the description. For node $i$ belonging to community $H_k$, the information resource quantity for individuals in state U is specifically defined as follows:

$$M^{\mathrm{U}}_{i\in H_k}(t) = \frac{\sum_j a_{ij}P^{\mathrm{A}}_j(t)M^{\mathrm{A}}_i(t)}{\sum_{l\neq i} a_{jl}P^{\mathrm{U}}_l(t)+2} + \gamma_1 F\left[\eta_1 - \frac{Q_i}{N}\right] + \gamma_2 F\left[\frac{N^{\mathrm{I}}_{H_k}(t)}{N_{H_k}} - \eta_2\right]. \tag{4}$$

### 2.2. Disease transmission process

Within a time step, an S-state individual $i$ is infected with probability $\beta_i(t)$, and an I-state individual $j$ recovers to state S with probability $\mu_j(t)$. Medical resources refer to the personnel, materials, and supplies required for epidemic response and control, and they play an important role in protecting susceptible populations and treating patients, thereby affecting these two probabilities. In this paper, we also use "unit" as the measure to quantify the volume of medical resources. Protective medical supplies, including masks and gowns, create a robust protective barrier that directly lowers an individual's chance of encountering pathogens. Meanwhile, vaccines and prophylactic drugs prime the immune system in advance, rendering susceptible individuals resistant to infection upon pathogen exposure. Consequently, for S-state individuals, the more medical resources they have, the more effectively they are protected from disease, thus reducing the infection rate. For I-state individuals, the more medical resources they have, the higher the likelihood that the disease will be cured, thus increasing the recovery rate. At time step $t$, the probability $\beta_i(t)$ of node $i$ being infected in the S-state and the probability $\mu_j(t)$ of node $j$ recovering in the I-state are defined as follows:

$$\mu_j(t) = 1-\mu\left(1-\varepsilon_3\right)^{R_j(t)}, \tag{5}$$

$$\beta_i(t) = \beta\varepsilon_4^{R_i(t)}. \tag{6}$$

In this context, $\mu$ denotes the level of accessibility of medical resources, where an increase in $\mu$ indicates greater difficulty in receiving medical resources. $\varepsilon_3$ and $\varepsilon_4$ represent the utilization rate of therapeutic medical resources and the utilization rate of preventive medical resources, respectively. $R_i(t)$ refers to the medical resources of node $i$ at time step $t$.




**Fig. 4.** SIS state transition diagram.

Medical resources are mainly accessed through S-state individuals and distributed within the community. An S-state individual generates one unit of medical resources within each time step, then divides this one unit of medical resources equally among its I-state neighbors. Meanwhile, all individuals in communities with infection rates exceeding $\eta_3$, namely high-risk communities, will receive one unit of medical resources from the community they belong to within a time step. It is also assumed that the medical resources received by an S-state individual from its community will not be distributed to its I-state neighbors.

Within each time step, the medical resource quantity of an S-state individual is: (i) one unit of medical resource generated by each S-state individual themselves (then the S-state individual divides this one unit of medical resources equally among I-state neighbors); (ii) S-state individuals in communities with an infection rate $N^{\mathrm{I}}_{H_k}(t)/N_{H_k}$ exceeding $\eta_3$ receive one unit of medical resource from their respective communities. For node $i$ belonging to community $H_k$, the medical resource quantity for S-state individuals is specifically defined as follows:

$$R^{\mathrm{S}}_{i\in H_k}(t) = \frac{1}{\sum_j b_{ij}P^{\mathrm{I}}_j(t)+1} + F\left[\frac{N^{\mathrm{I}}_{H_k}(t)}{N_{H_k}} - \eta_3\right]. \tag{7}$$

Within each time step, the medical resource quantity of I-state individuals is: (i) the sum of medical resources $(\sum_j b_{ij}P^{\mathrm{S}}_j(t))/(\sum_{l\neq i} b_{jl}P^{\mathrm{I}}_l(t)+2)$ shared by all S-state neighbors; (ii) I-state individuals in communities with an infection rate $N^{\mathrm{I}}_{H_k}(t)/N_{H_k}$ exceeding $\eta_3$ receive one unit of medical resource from their respective communities. For node $i$ belonging to community $H_k$, the medical resource quantity for I-state individuals is specifically defined as follows:

$$R^{\mathrm{I}}_{i\in H_k}(t) = \frac{\sum_j b_{ij}P^{\mathrm{S}}_j(t)}{\sum_{l\neq i} b_{jl}P^{\mathrm{I}}_l(t)+2} + F\left[\frac{N^{\mathrm{I}}_{H_k}(t)}{N_{H_k}} - \eta_3\right]. \tag{8}$$

### 2.3. Coupling effects of information and disease

When individuals have information about the disease, they will take certain precautions to reduce their risk of infection. Therefore, the probability of contracting the disease will be different depending on an individual's state in the information-dissemination layer, which in this paper is specifically represented by the difference in the initial infection rate. The initial infection rate of a U-state individual is defined as $\beta^{\mathrm{U}} = \beta$, and the initial infection rate of an A-state individual is defined as $\beta^{\mathrm{A}} = \varphi\beta$, where $\varphi$ is the infection decay factor ($\varphi \in [0,1]$).

In this paper, a U-state individual transitions from an unaware state U to an aware state A immediately after being infected with the disease and remains in state A during the illness. Thus, there are three states of nodes US, AS, and AI in the two-layer network, and there is no UI state. All parameters in this paper are defined in Table 1.

**Table 1.** Parameter definitions.

| Parameter | Definition |
|---|---|
| $\lambda_i(t)$ | Probability of node $i$ in state U being informed at time step $t$ |
| $\delta_j(t)$ | Probability of node $j$ in state A forgetting information at time step $t$ |
| $\beta_i(t)$ | Probability of node $i$ in state S being infected at time step $t$ |
| $\mu_j(t)$ | Probability of node $j$ in state I recovering at time step $t$ |
| $M_i(t)$ | Information resources of node $i$ at time step $t$ |
| $R_i(t)$ | Medical resources of node $i$ at time step $t$ |
| $\lambda$ | Accessibility level of information resources |
| $\delta$ | Initial information forgetting rate |
| $\beta$ | Initial infection rate |
| $\mu$ | Accessibility level of medical resources |
| $\varepsilon_1$ | Information assimilation utilization rate |
| $\varepsilon_2$ | Memory decay utilization rate |
| $\varepsilon_3$ | Utilization rate of therapeutic medical resources |
| $\varepsilon_4$ | Utilization rate of preventive medical resources |
| $\gamma_1$ | Decay factor for mass media information resource reception volume |
| $\gamma_2$ | Decay factor for community publicity information resource reception volume |
| $\varphi$ | Infection attenuation factor |
| $\eta_1$ | Node proportion of mass media propaganda information |
| $\eta_2$ | Community information resource activation threshold |
| $\eta_3$ | Community medical resource activation threshold |
| $Q_i$ | Degree ranking of node $i$ in the information dissemination layer |
| $N$ | Number of nodes at the information dissemination layer |
| $H_k$ | Community numbered $k$ |
| $N_{H_k}$ | Number of total nodes in community $H_k$ of the disease transmission layer at time step $t$ |
| $N^{\mathrm{I}}_{H_k}(t)$ | Number of infected nodes in community $H_k$ of the disease transmission layer at time step $t$ |

## 3. Theoretical analysis

This paper employs MMCA theory to analyze the coupled spreading dynamics in two-layer networks. Let $a_{ij}$ and $b_{ij}$ denote the adjacency matrices of the information dissemination layer and the disease transmission layer, respectively. If nodes $i$ and $j$ are connected in the information dissemination layer (or disease transmission layer), then $a_{ij}(b_{ij}) = 1$; otherwise, $a_{ij}(b_{ij}) = 0$.

The $r_i(t)$ denotes the probability that a U-state individual does not transition to state A at time step $t$, $q_i^{\mathrm{U}}(t)$ is the probability that a U-state individual is not infected, and $q_i^{\mathrm{A}}(t)$ is the probability that an A-state individual is not infected. These probabilities are defined as follows:

$$r_i(t) = \prod_j \left[1 - a_{ji} P_j^{\mathrm{A}}(t)\lambda_i(t)\right], \tag{9}$$

$$q_i^{\mathrm{U}}(t) = \prod_j \left[1 - b_{ji} P_j^{\mathrm{I}}(t)\beta_i^{\mathrm{U}}(t)\right], \tag{10}$$

$$q_i^{\mathrm{A}}(t) = \prod_j \left[1 - b_{ji} P_j^{\mathrm{I}}(t)\beta_i^{\mathrm{A}}(t)\right]. \tag{11}$$

We construct the probability trees for state transitions in Fig. 5.

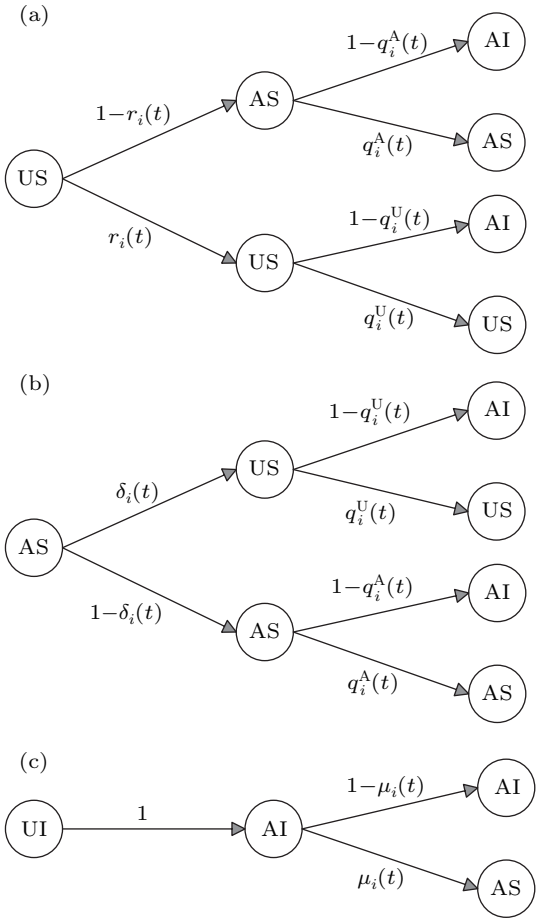



**Fig. 5.** Probability trees.

Based on the probability trees, we derive the state probability transition equations for node $i$ as

$$\begin{aligned} P_i^{\mathrm{AS}}(t+1) &= P_i^{\mathrm{US}}(t)\left(1-r_i(t)\right)q_i^{\mathrm{A}}(t) \\ &\quad + P_i^{\mathrm{AS}}(t)\left(1-\delta_i(t)\right)q_i^{\mathrm{A}}(t) + P_i^{\mathrm{AI}}(t)\mu_i(t), \end{aligned} \tag{12}$$

$$P_i^{\mathrm{US}}(t+1) = P_i^{\mathrm{US}}(t)\, r_i(t)\, q_i^{\mathrm{U}}(t) + P_i^{\mathrm{AS}}(t)\,\delta_i(t)\, q_i^{\mathrm{U}}(t), \tag{13}$$

$$\begin{aligned} P_i^{\mathrm{AI}}(t+1) &= P_i^{\mathrm{US}}(t)\Big[\left(1-r_i(t)\right)\left(1-q_i^{\mathrm{A}}(t)\right) \\ &\quad + r_i(t)\left(1-q_i^{\mathrm{U}}(t)\right)\Big] \\ &\quad + P_i^{\mathrm{AS}}(t)\Big[\delta_i(t)\left(1-q_i^{\mathrm{U}}(t)\right) \\ &\quad + \left(1-\delta_i(t)\right)\left(1-q_i^{\mathrm{A}}(t)\right)\Big] \\ &\quad + P_i^{\mathrm{AI}}(t)\left(1-\mu_i(t)\right). \end{aligned} \tag{14}$$

Near the epidemic threshold $\beta_{\mathrm{c}} = \beta_{\mathrm{c}}^{\mathrm{U}}$, where the proportion of infected nodes approaches zero, we assume $P_i^{\mathrm{A}} = P_i^{\mathrm{AI}} = \sigma_i \ll 1$. Equations (10) and (11) are approximated as

$$\begin{aligned} q_i^{\mathrm{U}}(t) &= \prod_j \left[1 - b_{ji} P_j^{\mathrm{I}}(t)\beta_i^{\mathrm{U}}(t)\right] \\ &\approx 1 - \beta_i^{\mathrm{U}}(t)\sum_j b_{ji}\sigma_j = 1 - \alpha_i, \end{aligned} \tag{15}$$

$$q_i^{\mathrm{A}}(t) = \prod_j \left[1 - b_{ji} P_j^{\mathrm{I}}(t)\beta_i^{\mathrm{A}}(t)\right]$$

$$\approx 1-\beta_i^{\mathrm{A}}(t)\sum_j b_{ji}\sigma_j = 1-\varphi\alpha_i, \tag{16}$$

where $\alpha_i = \beta_i^{\mathrm{U}}(t)\sum_j b_{ji}\sigma_j = \beta\varepsilon_4^{R_i(t)}\sum_j b_{ji}\sigma_j$.

As $t$ approaches infinity, $P_i^{\mathrm{AI}} = \sigma_i \ll 1$ and $\sigma_i$ is sufficiently small. Neglecting all higher-order terms in Eqs. (12) and (13), we obtain

$$P_i^{\mathrm{US}} = P_i^{\mathrm{US}} r_i + P_i^{\mathrm{AS}}\delta_i, \tag{17}$$

$$P_i^{\mathrm{AS}} = P_i^{\mathrm{US}}(1-r_i) + P_i^{\mathrm{AS}}(1-\delta_i). \tag{18}$$

Under steady-state conditions, Eq. (14) becomes

$$\begin{aligned}\sigma_i &= P_i^{\mathrm{US}}\left[(1-r_i)\varphi\alpha_i + r_i\alpha_i\right] + P_i^{\mathrm{AS}}\left[\delta_i\alpha_i + (1-\delta_i)\varphi\alpha_i\right] \\ &\quad +\sigma_i(1-\mu_i).\end{aligned} \tag{19}$$

Substituting Eqs. (17) and (18) into Eq. (19) yields

$$\begin{aligned}\sigma_i &= \sigma_i(1-\mu_i) + P_i^{\mathrm{US}}\alpha_i + P_i^{\mathrm{AS}}\varphi\alpha_i \\ &= \sigma_i(1-\mu_i) + \left(P_i^{\mathrm{US}} + P_i^{\mathrm{AS}}\varphi\right)\beta\varepsilon_4^{R_i}\sum_j b_{ji}\sigma_j.\end{aligned} \tag{20}$$

Since $P_i^{\mathrm{US}} + P_i^{\mathrm{AS}} + P_i^{\mathrm{AI}} = 1$ and assuming $P_i^{\mathrm{AS}} \approx P_i^{\mathrm{A}}$, $P_i^{\mathrm{US}} \approx 1 - P_i^{\mathrm{A}}$, Eq. (20) leads to

$$\mu_i\sigma_i = \left(1-(1-\varphi)P_i^{\mathrm{A}}\right)\beta\varepsilon_4^{R_i}\sum_j b_{ji}\sigma_j. \tag{21}$$

That is,

$$\sum_j\left\{\left[\left(1-(1-\varphi)P_i^{\mathrm{A}}\right)\varepsilon_4^{R_i}\right]b_{ji} - \frac{\mu_i}{\beta}e_{ij}\right\}\sigma_j = 0. \tag{22}$$

Let $h_{ji} = \left\{\left[1-(1-\varphi)P_i^{\mathrm{A}}\right]\varepsilon_4^{R_i}\right\}b_{ji}$, $B = [b_{ij}]$, then

$$H = \left\{\left[1-(1-\varphi)P_i^{\mathrm{A}}\right]\varepsilon_4^{R_i}\right\}B. \tag{23}$$

The critical threshold of the system can be characterized by the largest eigenvalue of matrix $H$, giving

$$\beta_{\mathrm{c}} = \frac{\mu_i}{\Lambda_{\max}(H)} = \frac{1-\mu(1-\varepsilon_3)^{R_i}}{\left\{\left[1-(1-\varphi)P_i^{\mathrm{A}}\right]\varepsilon_4^{R_i}\right\}\Lambda_{\max}(B)}. \tag{24}$$

## 4. Simulation

In this section, we employ Monte Carlo simulations to investigate the effects of various parameters on the epidemic threshold and outbreak size. The two-layer networks are configured with a size of $N = 1000$ and an average degree of $\langle k\rangle = 6$.[26,38,39] All simulation outputs correspond to the system reaching a steady state. In the $40\times 40$ gridded heatmaps, each grid value represents the average of 50 Monte Carlo simulation runs. The initial proportions of individuals in states A and I are both set to 0.1. Decay factors $\gamma_1$ and $\gamma_2$ (for different information resource reception volumes) are set to 0.4 and 0.6, respectively.

### 4.1. Impact of information resource on disease transmission

In this paper, the information assimilation utilization rate $\varepsilon_1$ refers to the efficiency with which an individual can effectively absorb and utilize information resources, while the memory decay utilization rate $\varepsilon_2$ pertains to the decline in an individual's capacity to retain and retrieve important information.

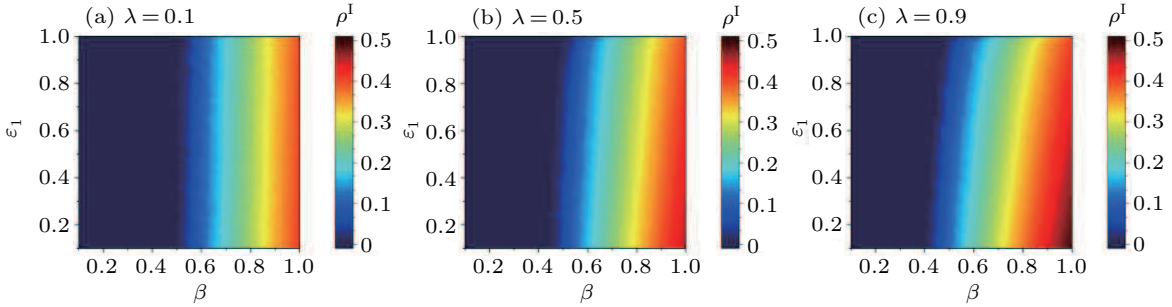



**Fig. 6.** $\rho^{\mathrm{I}}$ under different information assimilation utilization rates $\varepsilon_1$ and infection rates $\beta$. The other parameter settings are $\delta = 0.9$, $\mu = 0.5$, $\varphi = 0.5$, $\varepsilon_2 = 0.9$, $\varepsilon_3 = \varepsilon_4 = 0.1$, $\eta_1 = 0.2$ and $\eta_2 = \eta_3 = 0.8$.

In Fig. 6(a) with $\lambda = 0.1$, $\varepsilon_1$ has almost no impact on the threshold for disease outbreak or the scale of infection. However, in Figs. 6(b) and 6(c), where $\lambda$ is set to 0.5 and 0.9, respectively, a higher $\varepsilon_1$ leads to a larger outbreak threshold and a smaller scale of infection. Moreover, as $\lambda$ increases, the inhibitory effect of $\varepsilon_1$ on disease transmission becomes more pronounced. This is because when the accessibility level of information resources $\lambda$ is limited, information can already be disseminated widely and efficiently to most target populations. Although increasing the information assimilation utilization rate $(\varepsilon_1)$ enhances the effectiveness of information propagation, it does not significantly alter the behavior of individuals who have already received the information and adopted protective measures. Consequently, improving $\varepsilon_1$ has limited inhibitory effects on disease spread under such conditions. Conversely, when the accessibility level of information resources $(\lambda)$ is high, information cannot be comprehensively and accurately disseminated to the public. In such cases, it is nec-

essary to improve the information assimilation utilization rate by optimizing the format of the information content, thereby amplifying its propagation effects. For example, during the COVID-19 pandemic, strategies such as adapting classical poetry to encourage public participation in nucleic acid testing or organizing "epidemic prevention knowledge challenge" campaigns as trending topics significantly boosted public engagement and discussion, thereby enhancing the dissemination of pandemic control information.

Additionally, from Figs. 6(a) to Fig. 6(c), under the same $\varepsilon_1$, a larger $\lambda$ corresponds to a smaller disease outbreak threshold and a larger scale of infection. An increase in the accessibility level of information resources implies that the dissemination of disease-related information is hindered, thereby weakening the inhibitory effect on disease outbreaks. During the epidemic prevention and control phase, public access to official information channels is limited, particularly in remote areas with underdeveloped communication systems. Weak network infrastructure in these regions makes it challenging for the local population to receive mass media information. Authorities should address the insufficient coverage of preventive information by deploying emergency communication capabilities and strengthening the role of grassroots organizations and community workers.

Figure 7 shows the impact of the memory decay utilization rate ($\varepsilon_2$) on disease spread under varying accessibility levels of information resources ($\lambda$). Notably, an increase in $\varepsilon_2$ within the 0–0.4 interval is inversely correlated with the epidemic outbreak threshold, precipitating an amplified scale of disease spread. A high memory decay utilization rate exacerbates information overload in individuals, making it harder for them to retain critical protective measures and thereby increasing the risk of infection. Once $\varepsilon_2$ surpasses 0.4, the threshold for disease outbreaks and the scale of infection remain nearly unchanged. At this point, a high memory decay utilization rate indicates that public attention and memory capacity have reached saturation. The volume of information that people can retain does not increase and remains consistent with the scenario of a low memory decay utilization rate. This results in limited behavioral adjustments and negligible impact on disease transmission dynamics. In practice, authorities should refine information into concise formats to alleviate the public's cognitive burden, promoting the more efficient memorization of key messages. Additionally, the continuous reinforcement of critical information through repeated dissemination will help solidify public retention of vital epidemic prevention knowledge.

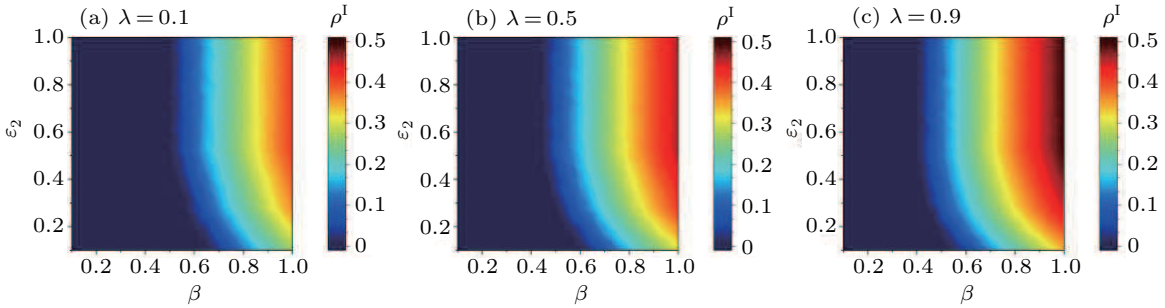



**Fig. 7.** $\rho^{\mathrm{I}}$ under different memory decay utilization rates $\varepsilon_2$ and infection rates $\beta$. The other parameter settings are $\delta = 0.9$, $\mu = 0.5$, $\varphi = 0.5$, $\varepsilon_1 = \varepsilon_3 = \varepsilon_4 = 0.1$, $\eta_1 = 0.2$ and $\eta_2 = \eta_3 = 0.8$.

### 4.2. Impact of medical resources on disease transmission

In this paper, the utilization rate of therapeutic medical resources $\varepsilon_3$ pertains to the efficiency of individuals in utilizing therapeutic medical resources that are employed for treating illnesses and are conducive to disease recovery. Meanwhile, the utilization rate of preventive medical resources $\varepsilon_4$ pertains to the efficiency of individuals in utilizing preventive medical resources that are intended for disease prevention and early intervention.

Figure 8 demonstrates that under varying accessibility levels of medical resources $\mu$, an increase in $\varepsilon_3$ elevates the disease outbreak threshold and reduces the scale of the disease. In other words, the more sufficient the therapeutic medical resources available to individuals, the better the treatment outcomes. This not only aids patient recovery and increases the number of cured individuals but also effectively prevents further disease transmission, enabling rapid control of the epidemic. Therefore, enhancing the utilization of therapeutic medical resources — through drug development, equipment upgrades, and optimized allocation of medical personnel — can shorten treatment duration and reduce disease transmission risks. From Fig. 8(a) to Fig. 8(c), when the utilization rate of therapeutic medical resources $\varepsilon_3$ is constant, a higher accessibility level of medical resources $\mu$ corresponds to a lower disease outbreak threshold and a larger scale of disease. This occurs because as $\mu$ increases, issues such as the uneven allocation of medical resources hinder the fulfillment of patients' treatment demands, resulting in a higher number of infected individuals in the network. To address this, govern-

ments should prioritize strengthening community-level medical infrastructure to reduce the accessibility level of medical resources, thereby effectively controlling disease transmission at the community level.

In Fig. 9, we observe that increasing $\varepsilon_4$ produces the opposite effect to increasing $\varepsilon_3$. This is because a higher utilization rate of preventive medical resources for disease prevention does not mean that resources are utilized efficiently. On the one hand, resource wastage — such as unnecessary examinations — deprives other patients in greater need of adequate treatment, exacerbating overall shortages of medical resources and hindering disease control. On the other hand, if preventive measures fail to effectively modify high-risk behaviors (such as gatherings, not wearing masks, and so on), the scale of the disease may still expand. Furthermore, as the difficulty in accessing medical resources increases, resources tend to concentrate in specific regions or groups, leaving other areas or populations with insufficient preventive measures. This creates conditions for localized outbreaks and subsequent spread. Therefore, when allocating preventive medical resources, greater emphasis should be placed on minimizing waste and improving the efficiency of resource allocation.

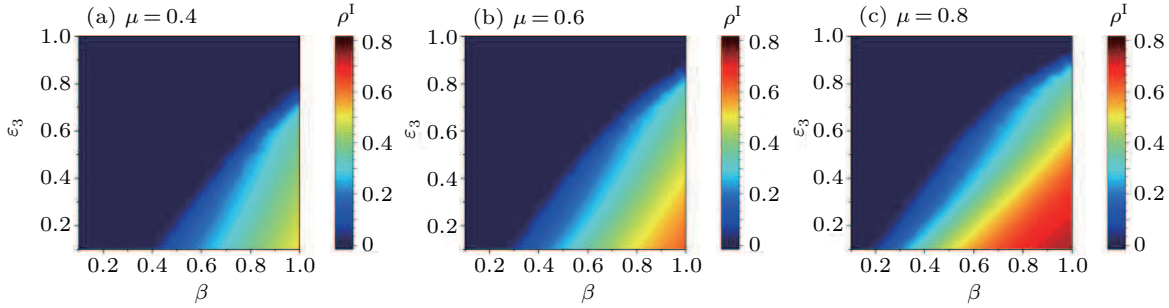



**Fig. 8.** $\rho^{\mathrm{I}}$ under different therapeutic medical resources utilization rates $\varepsilon_3$ and infection rates $\beta$. The other parameter settings are $\delta = 0.9$, $\lambda = 0.6$, $\varphi = 0.5$, $\varepsilon_1 = \varepsilon_2 = 0.1$, $\varepsilon_4 = 0.6$, $\eta_1 = 0.2$ and $\eta_2 = \eta_3 = 0.8$.

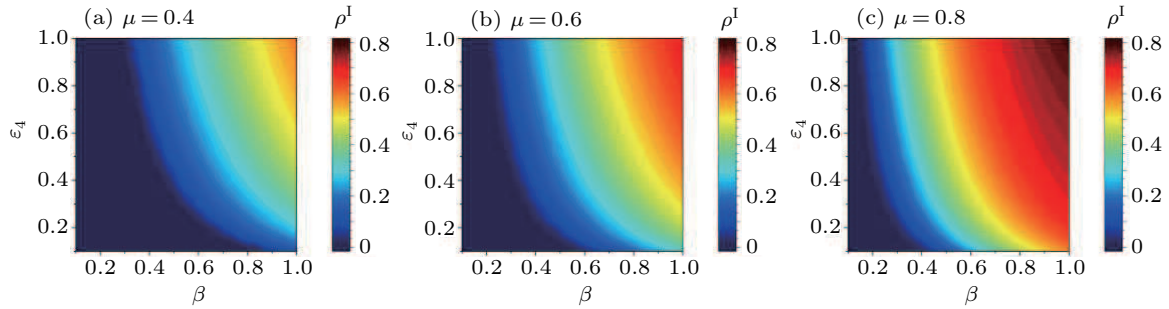



**Fig. 9.** $\rho^{\mathrm{I}}$ under different preventive medical resources utilization rates $\varepsilon_4$ and infection rates $\beta$. The other parameter settings are $\delta = 0.9$, $\lambda = 0.6$, $\varphi = 0.5$, $\varepsilon_1 = \varepsilon_2 = \varepsilon_3 = 0.1$, $\eta_1 = 0.2$ and $\eta_2 = \eta_3 = 0.8$.

### 4.3. Impact of resource allocation strategies in disease transmission

This paper establishes two sources of resource allocation, mass media and community, prioritizing the allocation of resources to degree-high nodes and high-infection communities.

#### 4.3.1. Impact of mass media propaganda on disease transmission

The mass media propaganda coverage $\eta_1$ represents the allocation of information resources to the top $\eta_1$ degree-ranked node information dissemination layers. Figure 10 demonstrates that as $\eta_1$ increases, the epidemic threshold rises, and the scale of infection decreases. With increased propaganda coverage by mass media, more individuals in the information dissemination layer gain knowledge about the disease. They then adopt protective measures to reduce the probability of infection, suppressing the spread of the disease. Therefore, during the disease prevention and control phase, the government should fully

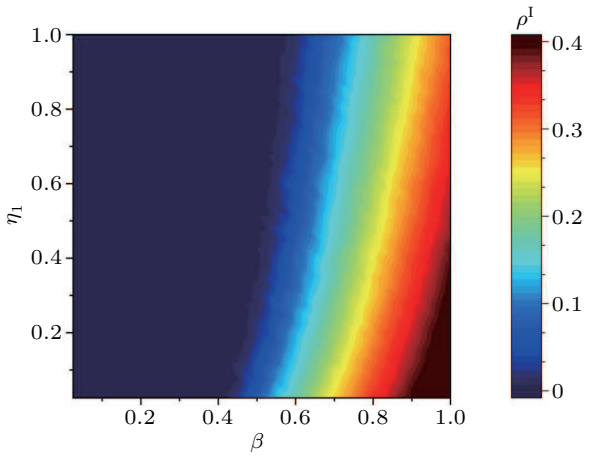



**Fig. 10.** $\rho^{\mathrm{I}}$ under different mass media propaganda coverages $\eta_1$ and infection rates $\beta$. The other parameter settings are $\delta = 0.9$, $\mu = 0.6$, $\varphi = 0.5$, $\varepsilon_1 = \varepsilon_2 = \varepsilon_3 = \varepsilon_4 = 0.1$, $\eta_2 = \eta_3 = 0.8$ and $\lambda = 0.8$.

utilize mass media to accurately target disease-related information to network opinion leaders with extensive social connections, and build an official social media platform with significant influence. These measures will help to achieve the maximum coverage and efficient dissemination of information, enhancing the awareness of the public to prevent the spread of the disease.

#### 4.3.2. Impact of community propaganda on disease transmission

Figure 11 illustrates the impact of the community information resource activation threshold $\eta_2$ on disease spread. When $\eta_2$ decreases within the range 0–0.2, the disease outbreak threshold progressively increases. Beyond $\eta_2 = 0.2$, the outbreak threshold stabilizes and no longer changes. Under high-infection-rate scenarios, the scale of infection exhibits a similar nonlinear change. When $\eta_2$ is below 0.4, the infection scale increases as the threshold $\eta_2$ rises. Once $\eta_2$ exceeds 0.4, the scale of infection remains almost constant. The community information resource activation threshold $\eta_2$ refers to the predetermined community infection rate at which public awareness campaigns and resource allocation are initiated. A lower $\eta_2$ enables earlier implementation of publicity measures, allowing residents who are unaware of the outbreak to be informed at an earlier stage and to take effective preventive actions. However, when this threshold is set too high (for example, beyond the critical point of 0.4), even if campaigns are launched, the golden window for intervention has already been missed. By this time, as the outbreak has already spread widely within the community, a large number of residents may have already been exposed, infected, and gained awareness of the disease. Consequently, post-outbreak information dissemination proves less effective in breaking transmission chains and fails to significantly alter the final scale of infection. Therefore, community-based prevention awareness campaigns should be initiated as early as possible during the initial outbreak phase, and this is particularly crucial in high-infection-rate scenarios.

#### 4.3.3. Impact of community assistance on disease transmission

Figure 12 illustrates the impact of the community medical resource activation threshold $\eta_3$ on disease spread. Our analysis reveals that both the disease scale and the outbreak threshold in Fig. 12 exhibit a critical threshold effect similar to that observed in Fig. 11. Specifically, when threshold $\eta_3$ falls below a critical value, the disease scale decreases with the reduction of $\eta_3$, while the outbreak threshold increases as $\eta_3$ declines. Beyond this critical value, both the disease scale and the outbreak threshold remain largely unchanged. This occurs because a sufficiently low medical resource activation threshold $\eta_3$ enables timely resource allocation during an outbreak's early stages, facilitating early detection, early treatment, and effective isolation of infected individuals, thereby reducing the scale of infection. It also ensures that susceptible individuals gain prompt access to medical resources, strengthening community-level disease prevention and reducing transmission opportunities.

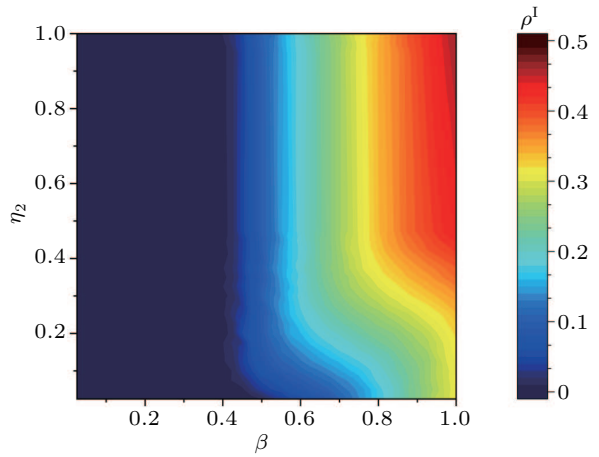



**Fig. 11.** $\rho^{\mathrm{I}}$ under different community information resource activation thresholds $\eta_2$ and infection rates $\beta$. The other parameter settings are $\delta = 0.9$, $\mu = 0.6$, $\varphi = 0.5$, $\varepsilon_1 = \varepsilon_2 = \varepsilon_3 = \varepsilon_4 = 0.1$, $\eta_1 = 0.01$, $\eta_3 = 0.01$ and $\lambda = 0.8$.

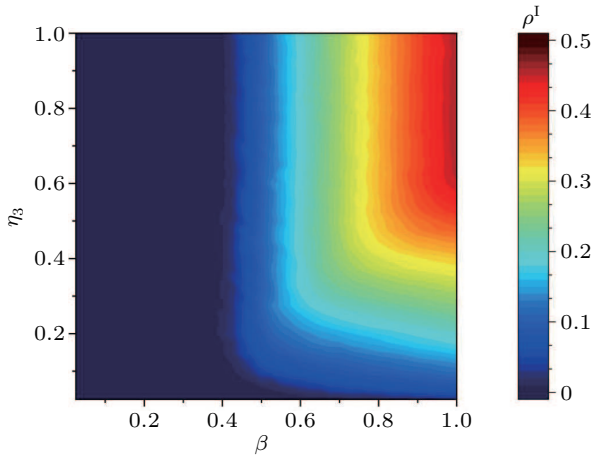



**Fig. 12.** $\rho^{\mathrm{I}}$ under different community medical resource activation thresholds $\eta_3$ and infection rates $\beta$. The other parameter settings are $\delta = 0.9$, $\mu = 0.6$, $\varphi = 0.5$, $\varepsilon_1 = \varepsilon_2 = \varepsilon_3 = \varepsilon_4 = 0.1$, $\eta_1 = 0.01$, $\eta_2 = 0.01$ and $\lambda = 0.8$.

More notably, we find that decreasing the threshold $\eta_3$ exerts a significantly stronger inhibitory effect on disease spread than reducing the threshold $\eta_2$ in Fig. 11. Under high transmission rates, epidemics fail to develop into large-scale outbreaks when the threshold $\eta_3$ remains within the range 0–0.2, whereas the scale of infection is larger within the same threshold range for $\eta_2$ in Fig. 11. This demonstrates that the allocation of medical resources in communities plays a more crucial role in epidemic control than publicity measures during the initial outbreak phase. While awareness campaigns influence protective behaviors among residents, the immediate availability of medical resources enables direct interventions — such as

case identification and treatment — that effectively interrupt transmission chains during the critical period.

### 4.4. Impact of coupling information and disease on disease transmission

When individuals are aware of information about a disease, they adopt various measures to reduce infection rates. In this paper, the infection attenuation factor $\varphi$ quantifies the extent to which an individual's infection rate decreases after acquiring such information. Figure 13 depicts the effect of the infection attenuation factor $\varphi$ and infection rate $\beta$. Figures 13(a)–13(c) collectively demonstrate that as $\varphi$ increases, the disease outbreak threshold decreases and the scale of the disease expands. A higher $\varphi$ indicates smaller differences in infection rates between aware and unaware individuals. When $\varphi = 1$, the infection rates of both groups become identical, meaning that awareness no longer mitigates disease transmission, leading to larger scales of infection. When $\varphi$ has a constant value, Figs. 13(a)–13(c) show that as the accessibility level of information resources increases, the disease outbreak threshold decreases and the scale of the disease grows. This aligns with the conclusions drawn from Fig. 6: a higher accessibility level of information resources weakens suppression of disease transmission. In public health campaigns, authorities should not only ensure the comprehensiveness and reliability of information but also enhance educational outreach and policy interpretation. By helping the public understand and adopt official recommendations — such as taking correct preventive measures, avoiding outbreak areas, and improving personal immunity — infection risks can be effectively reduced.

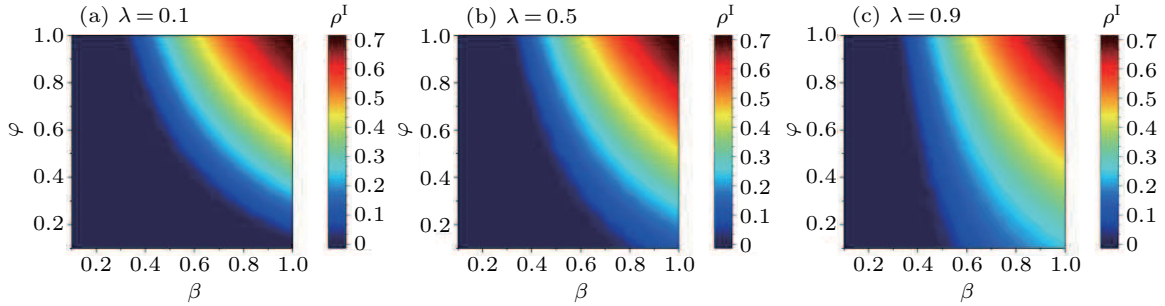



**Fig. 13.** $\rho^{\mathrm{I}}$ under different infection attenuation factors $\varphi$ and infection rates $\beta$. The other parameter settings are $\delta = 0.9$, $\mu = 0.6$, $\varepsilon_1 = \varepsilon_2 = \varepsilon_3 = \varepsilon_4 = 0.1$, $\eta_1 = 0.01$ and $\eta_2 = \eta_3 = 0.8$.

## 5. Conclusion

This study established a UAU–SIS two-layer network model to characterize the coupled propagation process of information and disease. By integrating both transmission dynamics, the model incorporates two sources of resource allocation: mass media and community interventions. A novel feature of the model is its consideration of node importance in resource distribution. Specifically, the prioritization of mass media allocating information resources to individuals with higher degree rankings in the information dissemination layer improves dissemination efficiency, while both information resources and medical resources are allocated to communities in regions with high infection rates, thereby suppressing disease spread in high-risk areas. The research employed the MMCA to derive the epidemic threshold and conducted Monte Carlo simulations to evaluate the impact of various parameters on disease spread. The results clearly indicate that intensifying mass media campaigns and lowering community intervention thresholds significantly increase the epidemic threshold and reduce the outbreak scale. Notably, community interventions should be initiated during the early stages of an outbreak, as resources allocated in later stages show limited effectiveness in controlling the epidemic, with medical resource investment demonstrating greater effectiveness than information resource allocation. In practical implementation, the government should intensify media campaigns to broaden information coverage while streamlining informational content, employing diverse formats to stimulate public engagement and discussion. Regarding medical resources, efforts must focus not only on rational allocation and improved accessibility but also on enhancing the utilization efficiency of therapeutic medical resources and preventing the waste of preventive medical resources. Future research should incorporate real-world datasets to construct more realistic network models, thereby improving the credibility and generalizability of the findings. In addition, systematic comparisons between simulated and empirical data will be conducted to iteratively optimize models and parameters, thereby providing more effective scientific strategies for controlling disease transmission.

## Acknowledgments

Project supported by the National Natural Science Foundation of China (Grant Nos. 72574145 and 72174121), the Program for Professor of Special Appointment (Eastern Scholar) at Shanghai Institutions of Higher Learning, and Project for the National Social Science Foundation of China

(Grant No. 21BGL217).

## References


[1] Lippi G and Sanchis-Gomar F 2025 *COVID* **5** 1
[2] Van den Borre L, Devleesschauwer B, Gadeyne S, *et al.* 2025 *Arch. Public Health* **83** 1
[3] Schumacher A, Kyu H, Aali A, *et al.* 2024 *Lancet* **403** 1989
[4] Ma Y and Wang J 2025 *Finance Res. Lett.* **71** 106390
[5] Faramarzi A, Norouzi S, Dehdarirad H, *et al.* 2024 *Syst. Rev.* **13** 1
[6] Zhu F, Yang Y, Yin T, *et al.* 2025 *Sci. Rep.* **15** 5658
[7] Chen Z, Tsui J, Cai J, *et al.* 2025 *Nat. Commun.* **16** 1
[8] Liu Z, Hu B, Zeng T, *et al.* 2025 *eBioMedicine* 105549
[9] Kermack W and McKendrick A 1927 *Proc. R. Soc. Lond. A* **115** 700
[10] Nekovee M, Moreno Y, Bianconi G, *et al.* 2007 *Physica A* **374** 457
[11] Gómez S, Arenas A, Borge-Holthoefer J, *et al.* 2010 *Europhys. Lett.* **89** 38009
[12] Granell C, Gómez S and Arenas A 2013 *Phys. Rev. Lett.* **111** 128701
[13] Granell C, Gómez S and Arenas A 2014 *Phys. Rev. E* **90** 012808
[14] Sun G, Mai A, Jin Z, *et al.* 2024 *Physica A* **652** 130064
[15] Zhu L, Ding Y and Shen S 2025 *Math. Biosci.* **379** 109340
[16] Bao H and He Y 2025 *Chaos* **35** 023135
[17] Yang T, Zhu L, Shen S, *et al.* 2025 *Math. Biosci.* 109502
[18] Han D and Wang X 2025 *Int. J. Mod. Phys. C* **36** 2450196
[19] Zhou H, Ma Y, Song L, *et al.* 2025 *Commun. Nonlinear Sci. Numer. Simul.* **153** 109466
[20] Liu L, Geng S, Wei L, *et al.* 2026 *Appl. Math. Comput.* **510** 129701
[21] Frieden T, Lee C, Lamorde M, *et al.* 2023 *Lancet Public Health* **8** 383
[22] Li J, Yang C, Ma X, *et al.* 2019 *Chaos* **29** 113108
[23] Wu Z and Pang S 2024 *Sci. Rep.* **14** 24523
[24] Chen X, Liu Q, Wang R, *et al.* 2020 *Complexity* **2020** 3256415
[25] Wang X, Zhu X, Tao X, *et al.* 2021 *Phys. Rev. Res.* **3** 013157
[26] Huo L and Zhao J 2024 *Nonlinear Dyn.* **113** 1953
[27] Yu Y and Huo L 2024 *Syst. Eng. Theory Pract.* **44** 3386 (in Chinese)
[28] Worby C and Chang H 2020 *Nat. Commun.* **11** 4049
[29] Meng X, Han S, Wu L, *et al.* 2022 *Reliab. Eng. Syst. Saf.* **219** 108256
[30] Chen X, Cai S, Tang M, *et al.* 2018 *Chaos* **28** 123116
[31] Wang R, Chen X and Cai S 2019 *Physica A* **533** 121968
[32] Liu Y, Zeng Q, Pan L, *et al.* 2023 *IEEE Trans. Netw. Sci. Eng.* **10** 2201
[33] Xian J, Zhang Z, Li Z, *et al.* 2023 *Entropy* **25** 1
[34] Pöyry E, Reinikainen H and Luoma-Aho V 2025 *Strategic Communication and the Global Pandemic* (Routledge) pp. 118–134
[35] Tripp C, Jensen T and Carlson L 1994 *J. Consum. Res.* **20** 535
[36] Powell R, Oladipupo B, Evans D, *et al.* 2024 *J. Emerg. Manag.* **22** 23
[37] Sesay U, Sheriff S and Osborne A 2025 *Discov. Health Syst.* **4** 35
[38] Hu X, Chen J and Xia C 2024 *Chin. Phys. B* **33** 100202
[39] Xie X, Huo L, Dong Y F, *et al.* 2024 *Chin. Phys. B* **33** 038704